



Strategic protection of landslide vulnerable mountains for biodiversity conservation under land-cover and climate change impacts

Binbin V. Li^{a,b,1} , Clinton N. Jenkins^{c,d} , and Weihua Xu^e

^aEnvironmental Research Centre, Duke Kunshan University, Jiangsu 215316, China; ^bNicholas School of the Environment, Duke University, Durham, NC 27708; ^cDepartment of Earth and Environment, Florida International University, Miami, FL 33199; ^dKimberly Green Latin American and Caribbean Center, Florida International University, Miami, FL 33199; and ^eState Key Laboratory of Urban and Regional Ecology, Research Center for Eco-Environmental Sciences, Chinese Academy of Sciences, Beijing 100085, China

Edited by Nils Stenseth, CEES, Department of Biosciences, Universitetet i Oslo, Oslo, Norway; received July 21, 2021; accepted October 29, 2021

Natural disasters impose huge uncertainty and loss to human lives and economic activities. Landslides are one disaster that has become more prevalent because of anthropogenic disturbances, such as land-cover changes, land degradation, and expansion of infrastructure. These are further exacerbated by more extreme precipitation due to climate change, which is predicted to trigger more landslides and threaten sustainable development in vulnerable regions. Although biodiversity conservation and development are often regarded as having a trade-off relationship, here we present a global analysis of the area with co-benefits, where conservation through expanding protection and reducing deforestation can not only benefit biodiversity but also reduce landslide risks to human society. High overlap exists between landslide susceptibility and areas of endemism for mammals, birds, and amphibians, which are mostly concentrated in mountain regions. We identified 247 mountain ranges as areas with high vulnerability, having both exceptional biodiversity and landslide risks, accounting for 25.8% of the global mountainous areas. Another 31 biodiverse mountains are classified as future vulnerable mountains as they face increasing landslide risks because of predicted climate change and deforestation. None of these 278 mountains reach the Aichi Target 11 of 17% coverage by protected areas. Of the 278 mountains, 52 need immediate actions because of high vulnerability, severe threats from future deforestation and precipitation extremes, low protection, and high-population density and anthropogenic activities. These actions include protected area expansion, forest conservation, and restoration where it could be a cost-effective way to reduce the risks of landslides.

landslides | biodiversity | mountain | climate change | priority setting

Land-cover/land-use changes, such as deforestation, agriculture expansion, and urbanization, are among the biggest drivers of biodiversity loss (1–3). These changes not only result in the decline of wildlife populations and fragmentation of habitats, but they also increase environmental risks, such as erosion of fertile soil and increases in avalanches, landslides, and flooding, especially in mountainous areas (4, 5). Landslides are one of the most prevalent natural hazards and are caused by changes in slope stability resulting from undercutting, changes in water saturation, or loss of woody vegetation (6). They have become more frequent because of anthropogenic activities and land-cover/land-use changes (7–9). Deforestation, infrastructure construction, and mining triggered about 16% of fatal landslides from 2004 to 2016 (10). Landslides cause direct and indirect damages worth billions of dollars each year across the world, contributing to 17% of the fatalities due to natural hazards (11). From 2006 to 2015, landslides alone accounted for 27.6% of the geological disasters worldwide and caused casualties of 9,477 people, threatening the livelihood of local communities (12).

While land-cover changes exacerbate the conditions for landslide activities, precipitation is the primary trigger for

landslides; one expected to increase in importance under climate change (13, 14). Either high-intensity, short-duration rainfall or prolonged rain at relatively low intensities can trigger landslides, creating a rainfall intensity–duration relationship for identifying possible areas of risk (15). Both model studies and historical records show an increase in precipitation extremes, such as heavy rainfall, flooding, and droughts with climate warming due to increases in the saturation vapor pressure of water (16–19). Consequently, the total precipitation from extreme events doubles per degree of warming, mainly because of increasing event frequencies (19). With this greater frequency and magnitude of heavy precipitation (20), landslides are expected to increase (21). For example, High Mountain Asia is predicted to experience a 30 to 70% increase in landslide activity because of the intensification of precipitation extremes (22). This geohazard poses one of the greatest threats of climate change to human safety and development with potentially huge economic losses (14).

It is crucial to understand the relationship between environmental risks, biodiversity, and the potential for sustainable development. This is true especially for mountain communities, where many people are in poverty and have low resilience and

Significance

Landslides are triggered more often by human-induced changes, such as deforestation, infrastructure building, and increasing precipitation extremes, because of climate change. The huge economic and societal loss calls for a more cost-effective way to reduce risks and ensure sustainable development. Land-cover and land-use changes not only increase landslide susceptibility but also drive habitat loss and species extinctions. The high spatial overlap between landslide susceptibility and biodiversity in mountains provides an opportunity to achieve co-benefits in conservation and development. The identification of vulnerable mountains with both high biodiversity and landslide susceptibility prioritizes the regions for expansion of protected areas, forest conservation, and restoration, providing a nature-based solution to mitigate landslide risks through the protection of natural habitat.

Author contributions: B.V.L. and C.N.J. designed research; B.V.L. performed research; B.V.L., C.N.J., and W.X. analyzed data; B.V.L. wrote the paper; and C.N.J. and W.X. revised the paper.

The authors declare no competing interest.

This article is a PNAS Direct Submission.

This open access article is distributed under [Creative Commons Attribution-NonCommercial-NoDerivatives License 4.0 \(CC BY-NC-ND\)](https://creativecommons.org/licenses/by-nc-nd/4.0/).

¹To whom correspondence may be addressed. Email: Binbin.li@dukekunshan.edu.cn.

This article contains supporting information online at <http://www.pnas.org/lookup/suppl/doi:10.1073/pnas.2113416118/-/DCSupplemental>.

Published January 3, 2022.

adaptive capacity (6, 22–24). About 24% of the global land area is mountains with 12% of the world’s population (25). Local communities directly depend on mountainous resources for their livelihoods and well-being (26). Residents in mountain areas are among the most economically vulnerable populations because of inaccessibility to markets and high risks from natural disasters, such as earthquakes, flash floods, and the impacts of climate change (25). However, the common development pattern relies on land-use changes and infrastructure building, which could pose higher environmental risks in mountainous areas than in lowland regions. For example, the expansion of road networks degrades the slope stability and further increases the susceptibility to landslides (27–29).

Mountain building driven by plate tectonics and volcanism provokes many geological disasters, including earthquakes, landslides, and volcanic movements (5, 30), but it also creates the landscape and climatic variations that drive species diversification. Mountains harbor an exceptionally large portion of the world’s biodiversity, including more than 85% of the world’s amphibian, bird, and mammal species (31). The interaction between speciation, coexistence, and persistence of species has resulted in high-species richness and endemism in most mountains, especially in the tropics (31). Nonetheless, habitat loss and degradation continue to threaten biodiversity in mountain regions, with increasing anthropogenic activities such as logging, livestock grazing, and agriculture expansion with a higher rate of land abandonment than lowland areas (32). Instead of trade-offs between conservation and development (33–35), we suggest that, with careful conservation planning and priority setting, a compatible outcome can be achieved. We identify vulnerable mountain regions for conservation that have both high biodiversity and landslide susceptibility. Since future landslide activity is expected to increase in areas with 1) increased deforestation and 2) increased regional precipitation due to climate change (36, 37), we also identified emerging vulnerable mountains in the future as priorities for conservation using land-use projections and climate scenarios. The emerging strategy of nature-based solutions (NBS) promotes nature as the means

for providing solutions to societal challenges (38, 39). Here, we present a potential NBS and identify key areas with the greatest potential to reduce landslide risks while also protecting biodiversity through expanding protected areas, reducing deforestation, and restoring forests.

Results

The Overlap between Biodiversity and Landslide Susceptibility. We used terrestrial vertebrate species, including mammals, birds, and amphibians, as our representative for biodiversity (40). We calculated and mapped rarity-weighted richness globally, which prioritizes regions with high numbers of limited range species and sometimes is identified as weighted endemism (41, 42). Mammals, birds, and amphibians followed a similar distribution pattern of this biodiversity metric (Fig. 1 A–C). Areas with the highest-rarity scores (>90th percentile) concentrate in mountainous areas across the globe, such as the Sierra Nevada in North America; the Sierra Madre in Central America; Andes and Brazilian East Coastal Range in South America; Himalayas, Ghats, and Hengduan Mountain Ranges in Asia; Barisan and Apokayan Ranges, Sulawesi, and Papua Highlands in Southeast Asia; the Drakensberg in Africa; and the Great Dividing Range in Australia. Some lowland regions also harbored a rich diversity of small-ranged species, such as coastal Madagascar.

To locate regions with high-landslide susceptibility, we used a global landslide susceptibility map that integrated five explanatory variables affecting the chances of landslide events, including slope, distance to faults, geological classification, presence of roads, and forest loss (28). The “very high” and “high” landslide susceptibility areas follow closely the distribution of mountains as well (Fig. 1D). Southeast Asia, the Himalayas, the west coast of North America, and the Andes in South America were shown as epicenters for landslides. Considering levels of protection, a higher proportion of the very high and high landslide susceptible areas were covered by protected areas, having 13.4 and 12.4% protected, respectively, compared to lower-risk areas (moderate landslide susceptible areas: 9.1%, low: 6.3%, and very low 6.1%).

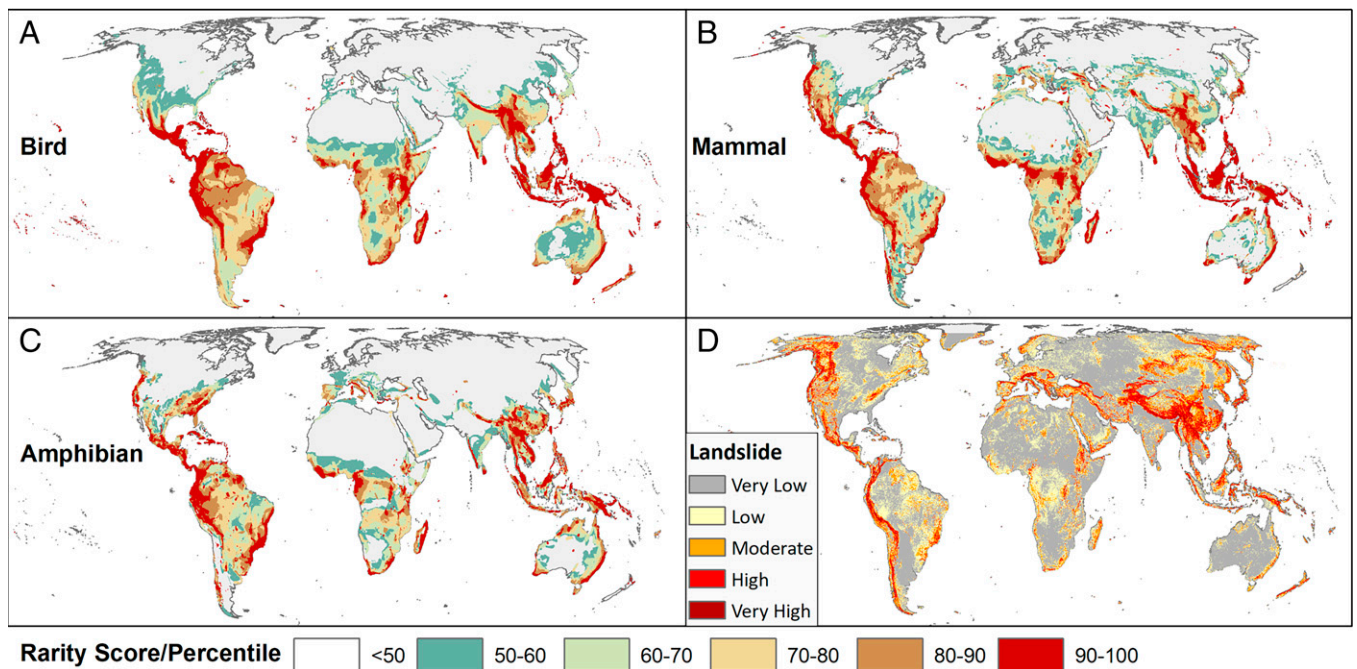


Fig. 1. Distribution of rarity-weighted richness and landslide susceptibility. Rarity-weighted richness is shown in six categories for birds (A), mammals (B), and amphibians (C). Values below the median are not shown. From the median to the 100th percentile, the values are divided into five equal intervals. (D) Landslide susceptibility is shown in five categories from Very Low to Very High.

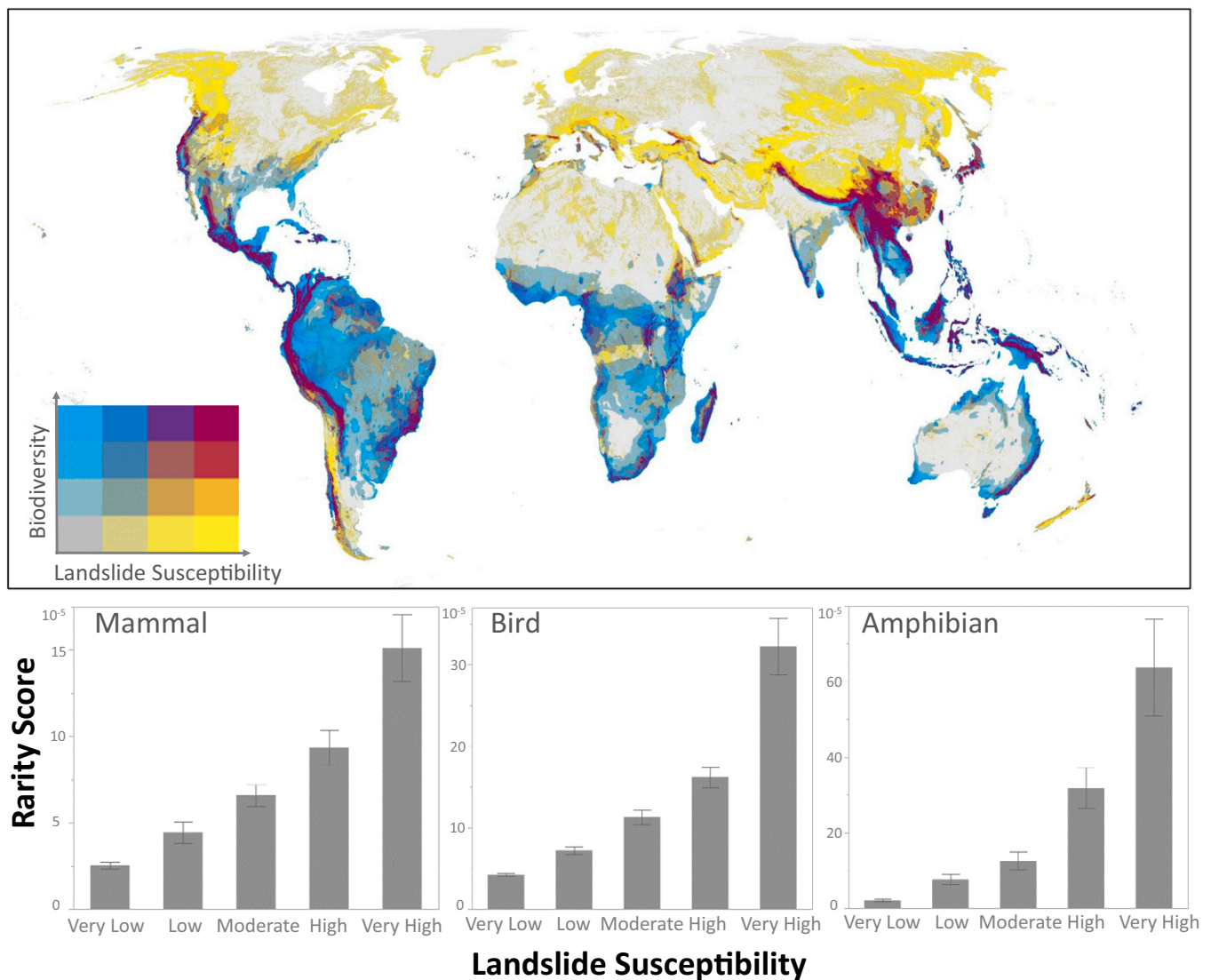


Fig. 2. Map of the relationship between multitaxa rarity score and landslide susceptibility. Graphs in the second row show the distribution of rarity-weighted richness in different landslide susceptibility zones.

There is a strong spatial correlation between the rarity-weighted richness and landslide susceptibility. The highest-endemism concentrates in the highest-landslide susceptibility areas (Fig. 2) and the average rarity score increases with the landslide susceptibility score ($P < 0.05$, t test) (Fig. 2). The most susceptible areas for landslides have 6 times the rarity-weighted richness of the least-susceptible areas for mammals, 8 times for birds, and 24 times for amphibians.

The areas with the highest overlaps between rarity-weighted richness and very high landslide susceptibility occur in Asia, including Himalaya and Hengduan Mountains in China, Western Ghat in India, the Barisan Mountains in Sumatra, Northern Borneo, and Papua New Guinea. The Northern Andes, west coast of Central America and North America, are also shown to be areas with high biodiversity and landslide risk. Comparatively, Africa, Europe, and Oceania have relatively few such areas (Fig. 2). The disparity between biodiversity and landslide susceptibility mainly concentrates in Alaska, Canada, Russia, West Europe, and New Zealand, which are high in landslide susceptibility but low in biodiversity. Conversely, the Amazon, lowland Africa, and coastal Australia showed the opposite, with high biodiversity but relatively low-landslide susceptibility.

Mountains with Vulnerability. We defined mountains with vulnerability as those with both high biodiversity and high-landslide susceptibility. This status was assigned to mountains with both biodiversity and landslide scores larger or equal to 4 (*SI Appendix, Table 1*). These areas are exceptionally sensitive to anthropogenic activities such as deforestation, agriculture expansion, and infrastructure building, which not only lead to biodiversity loss but also expose people to a higher probability of landslides.

Our assessment identified 247 mountain ranges with vulnerability, which we call current priorities in this study (Fig. 3). They harbor extremely high endemism (biodiversity score ≥ 4) while also facing a high-landslide susceptibility (landslide score ≥ 4). These mountains concentrate more in Asia and the Americas (Fig. 4A). Among them, China ranks the top with 36 mountains, followed by the United States with 22 mountains and Argentina with 13. Together, these 247 mountains accounted for 25.8% of the global mountainous areas. However, on average, these mountains had a significantly lower coverage of protected areas than other mountains ($11.3 \pm 16.4\%$ versus $13.7 \pm 21.7\%$, one-tail t test, $P = 0.035$). About 28.3% ($n = 70$) of these mountains have no protection and an additional 36.4% ($n = 90$) have less

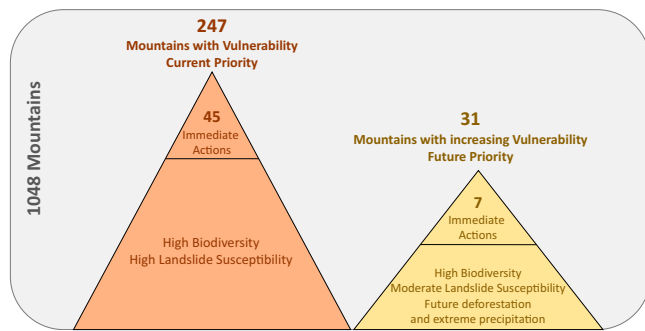


Fig. 3. Classification of different mountains. *Top* shows the number and definition of mountains with vulnerability, which are current priorities (247 mountains), as well as the mountains with increasing vulnerability that are future priorities (31 mountains). For each category, 45 and 7 mountains are needing immediate actions, a total of 52 mountains.

than 10% coverage by protected areas (red in Fig. 44). Only 23.5% ($n = 58$) of these vulnerable mountains reached the Aichi target, which was 17% coverage by 2020. These mountains are mostly in China ($n = 9$), the United States ($n = 9$), Colombia ($n = 6$), Venezuela ($n = 6$), and Japan ($n = 5$).

Threats from Future Change.

Deforestation. We calculated the deforestation rate from 2000 to 2018 using Global Land Cover Maps version 2.1 (43) and future forest loss using the land-cover projection from Li et al. (44). About 460 out of 1,048 mountains experienced forest loss from 2000 to 2018, with a deforestation rate of $1.5 \pm 2.2\%$ of the total area. Among these mountains, 96 are mountains with vulnerability, which also have a higher mean deforestation rate of $1.8 \pm 3.2\%$. The Santa Monica mountain range and Santa Ana mountain range in the United States ranked the top for forest loss among the vulnerable mountains, with a loss of 20.6 and 18.3% of its area between 2000 and 2018. More than half of the 1,048 mountains in the world are predicted to lose forests in the future, with 505 predicted to have a forest loss larger than 1%, while only 188 mountains are predicted to have a forest gain larger than 1% (Fig. 5). The highest deforestation rate (50 to 100% forest loss) would occur in mountains in South America along the Andes, Venezuela, and Atlantic Forest in Brazil; Parahyangan Highlands in Indonesia; Gogurock Range in Australia; Murat Dagi in Turkey; and various mountains in New Zealand. Increases in forest coverage would be mainly concentrated in mountains in Africa, Canada, Alaska, Russia, and several other countries in Europe.

Future forest loss continues to threaten the mountains with vulnerability, with 17 of the 247 currently vulnerable mountains projected to undergo a 50 to 100% forest loss. The majority of these ($n = 14$) are located in Latin America. Another 55 of 247 vulnerable mountains (22.3%) would experience a forest loss of 20 to 50%, 13.8% of the mountains have a loss of 10 to 20%, and 26.3% experience a loss smaller than 10%. In total, about 70% of the vulnerable mountains face continuing deforestation that would threaten the survival of biodiversity and further increase landslide susceptibility. For the mountains that would experience deforestation in the future, vulnerable mountains have less coverage by protected areas than the others ($12.0 \pm 15.5\%$ versus $16.5 \pm 24.1\%$, t test, $P = 0.011$). Especially for areas with deforestation rates higher than 20%, these vulnerable mountains have only half of the protected area coverage of the other mountains ($13.6 \pm 17.3\%$ versus $25.6 \pm 32.0\%$, t test, $P = 0.003$). This indicates a huge need to improve protected area coverage in the vulnerable mountains to resist deforestation.

Increasing precipitation extremes. Either high-intensity, short-duration rainfall or prolonged rain at relatively low intensities

can trigger landslides. This creates a rainfall intensity–duration relationship for identifying possible risks of landslides (15). We used the following precipitation extreme indices, RX5day, R95p, ALTCWD, and R20mm, to represent different measurements of duration and intensity and to indicate potential risks for landslides (45–47). We analyzed if there was a significant increase in each index between two periods, 1980 to 2019 and 2061 to 2100.

For the precipitation indices, 580 of the total 1,048 mountains showed a significant increase in RX5day, 513 mountains in R95p, 69 mountains in ALTCWD, and 26 mountains in R20mm (Fig. 5). Only Coxilha Grande in Brazil displayed significant increases in all the above precipitation extreme indices, but 75 mountains had three out of four indices showing a significant increase. Among them, Russia ranked the top for having 28 mountains listed, followed by Argentina (10 mountains), China (7 mountains), and the United States (5 mountains).

About 53.8% of the 247 mountains with current vulnerability would experience increasing precipitation extremes. A total of 12 mountains showed a high consistency between different precipitation extreme indices, with three or more precipitation extreme indices showing a significant increase, indicating an increase in the intensity, frequency, and duration of these events. Among them, mountains in Argentina and its bordering areas with Bolivia ($n = 5$) and Brazil ($n = 3$) had the most mountains with increasing extreme events. Other high-climate change risk mountains included Arakan Yoma in Myanmar, Bangma Shan in China and Myanmar, Boven Kapuas Mountains in Malaysia and Indonesia, and Central Range in Papua New Guinea.

Mountains with Increasing Vulnerability in the Future. We further considered mountains with high biodiversity (biodiversity score ≥ 4) and moderate-landslide susceptibility ($=1$ or 3) as candidates for mountains with increasing vulnerability in the future, as these mountains would have growing changes in forest cover and precipitation (Fig. 3). For these candidates, if the predicted forest loss was larger than 10% of the area, then it was identified as a mountain with increasing vulnerability in the future. If the forest loss was between 1 to 10% but the precipitation extreme indicator ≥ 2 , then it was identified as a mountain with increasing vulnerability as well.

In total, we identified 31 mountains with increasing vulnerability in landslides due to deforestation and climate change (Fig. 4B). Among them, 23 were in Latin America, including 10 mountains in Venezuela. Another two were in Australia, including Tasmania and Gogurock Range. Western Ghat in India; Central Highlands in Sri Lanka; the Chuor Phnum Kravanh in Cambodia; Phi Pan Nam Range in the bordering area between Laos, Myanmar, Thailand, the Sierra Madre Oriental in Mexico; and Albertine Rift Mountains in Africa were listed as mountains with high-future vulnerability. Twenty-eight mountains entered into this pool because of a predicted loss of at least 10% of the forest before 2100. Another three mountains were expected to experience a lower forest loss but with more precipitation extremes, including the Sierra Madre Oriental, Albertine Rift Mountains, and Serra da Espinhaco in Brazil. The average protected area coverage for these 31 mountains with increasing vulnerability was $17.1 \pm 24.8\%$. Although this was higher than the average for all mountains, which was $13.1 \pm 20.6\%$, five mountains had no protected areas at all, with an additional nine mountains having less than 10% coverage.

Key Mountains for Immediate Actions. We identified the 247 mountains with vulnerability in biodiversity and landslides as current priorities and 31 mountains with increasing vulnerability due to climate change and deforestation as future priorities. In total, 45 current priority mountains and 7 future priority mountains

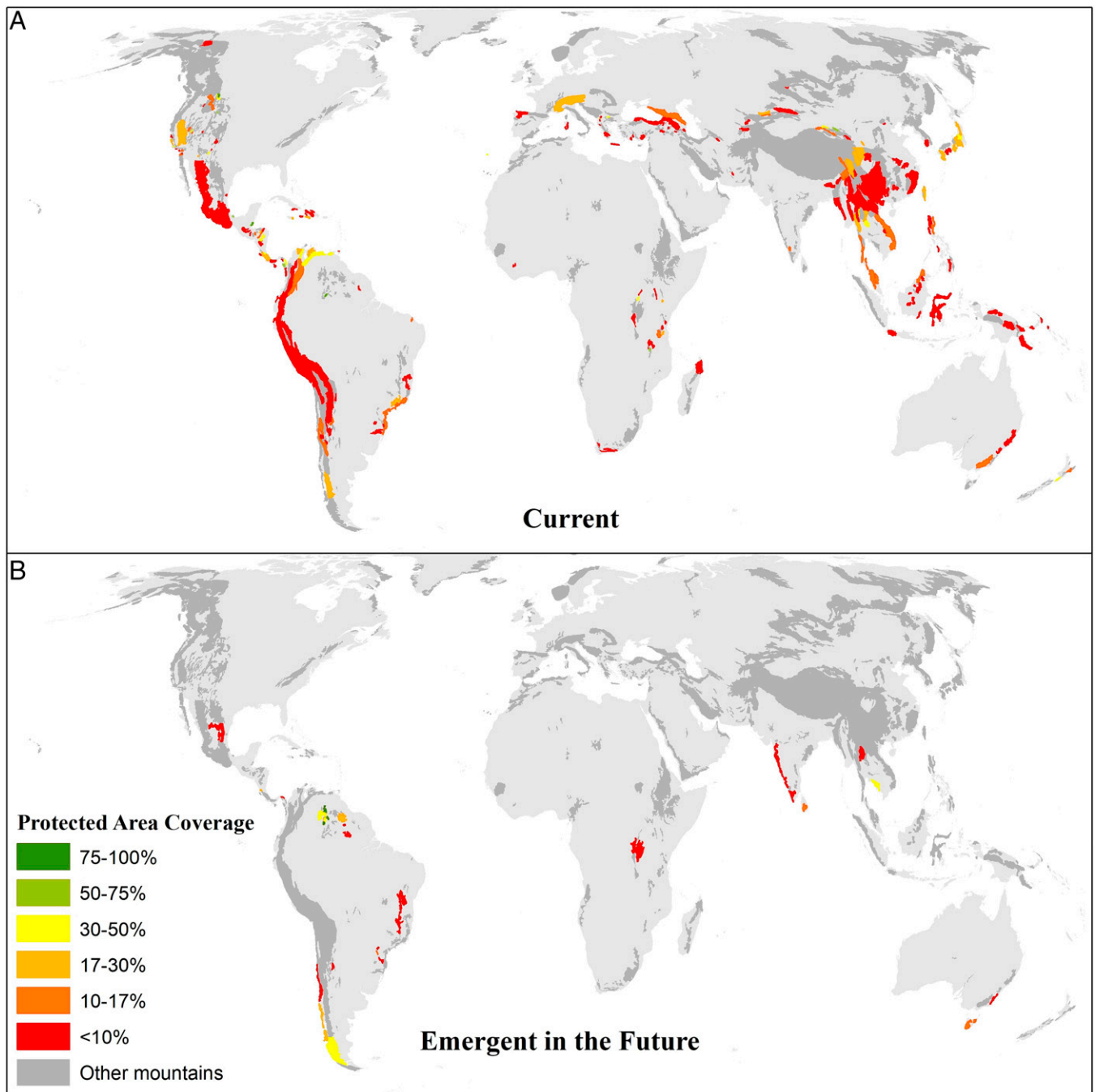


Fig. 4. Mountains with vulnerability and their protected area coverage. The mountains with vulnerability now ($n = 247$) (A) and the ones emerging with increasing vulnerability in the future ($n = 31$) (B). Mountains are shown in different colors (red to green) representing their current protected area coverage. Dark gray areas are mountains not identified as vulnerable.

would experience a forest loss larger than 10% and increasing precipitation extremes (precipitation extreme indicator ≥ 2) but with less than 17% of the area protected. We highlight these 52 mountains as key mountains for immediate actions (Figs. 3 and 6). These actions should address the deforestation problem, protecting the slope stability and biodiversity at the same time, which include protected area expansion, forest conservation, and restoration. Importantly, these mountains had a higher-human population density than the other mountains (Fig. 6D). The 45 current priority mountains have a mean population density of 101.9 person/km² (SD: 88.8), and it is 70.0 person/km² (SD: 123.8) for the seven future priority mountains. This compares to a lower density

of 57.2 person/km² (SD: 123.3) for the rest of the mountains (one-way ANOVA, $F = 2.92$, $P = 0.055$). Similarly, these priority mountains also showed a higher-human footprint index (48) than the rest (one-way ANOVA, $F = 8.07$, $P = 0.0003$) (Fig. 6E). The larger population density and anthropogenic changes (urbanization, agriculture, etc.) indicate a higher vulnerability to potential hazards with more economic loss and fatalities.

Discussion

The large spatial overlap between high biodiversity and landslide susceptibility in mountainous areas indicates a strong

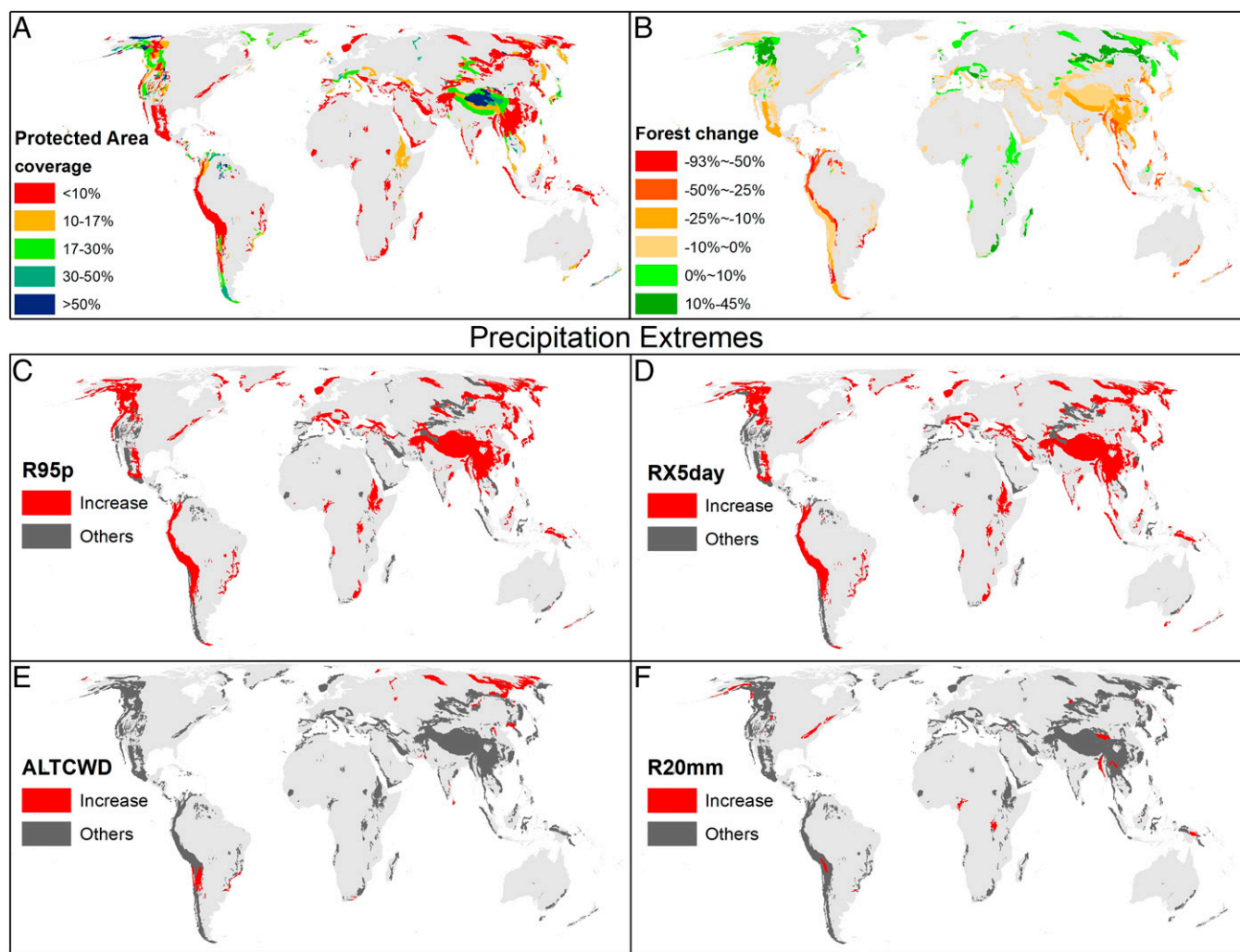


Fig. 5. Current protected area coverage (A), forest cover change projection (B), and precipitation extreme projections (C–F) into the year 2100 in mountains. (A) Protected area coverages are grouped into five categories, indicating different international conservation targets. (B) Forest cover change comparing 2100 to 2010. (C–F) Red areas indicate mountains with significant increases in the four precipitation extreme indices.

need to improve the protection of natural vegetation, especially forests. Forests not only provide critical ecosystem services and habitat for many species but their root matrix also holds soil in place and improves slope stability, thus reducing geological hazards and mitigating landslides (5). As our results show, most of the mountains with extremely high biodiversity and landslide susceptibility are expected to experience deforestation and increasing precipitation extremes, leading to greater landslide risks. Currently, these mountains have low coverage by protected areas, which is an important measure to resist land-cover/land-use changes and biodiversity loss.

Besides protecting existing forests and reducing future deforestation, forest restoration should also be prioritized in these vulnerable regions. Landslides are more likely to occur in non-forested lands and cause repeated damages to roads, pipelines, and buildings (5). The accumulative repair cost can be enormous in landslide-prone areas. Studies have shown that restoring forests in the Colombian Andes is 16 times more cost effective than repairing damaged infrastructure (5). As the United Nations has named 2020 to 2030 as the decade for restoration, mountains with high vulnerability should be prioritized for forest restoration for both mountainous biodiversity and their human residents. Nonetheless, some fast-growing, exotic tree species should be avoided for restoration, not only

because of their low contribution to biodiversity and negative impacts on ecosystems but also their shallow root system makes those less effective in stabilize the slopes (51–53).

The conflict between conservation and development is compounded by the fact that socioeconomic development is a key issue in mountain regions; most populations are in poverty (6, 24). Thus, mountainous areas should address sustainable development more than other areas because of their vulnerability, high-disaster risks and the impacts of climate change. Traditional development model which relies on land-cover and land-use changes and heavy infrastructure building should be avoided or planned more strategically to reduce environmental risks (49, 50). Old villages and settlements are usually located in relatively safe spots, although natural disasters could still happen episodically. However, new settlements and infrastructure tend to be expanded to areas farther from these safe places into areas with high risks. Human disturbances and climate change further intensify hazard conditions. Alternatively, by restricting infrastructure building that disturbs slope stability and protecting areas to reduce deforestation and other land-cover changes, local communities could achieve more sustainable development without spending huge resources in disaster recovery. As most of the priority mountains that we identified do not reach the Aichi target for protection, further expansion of protected areas

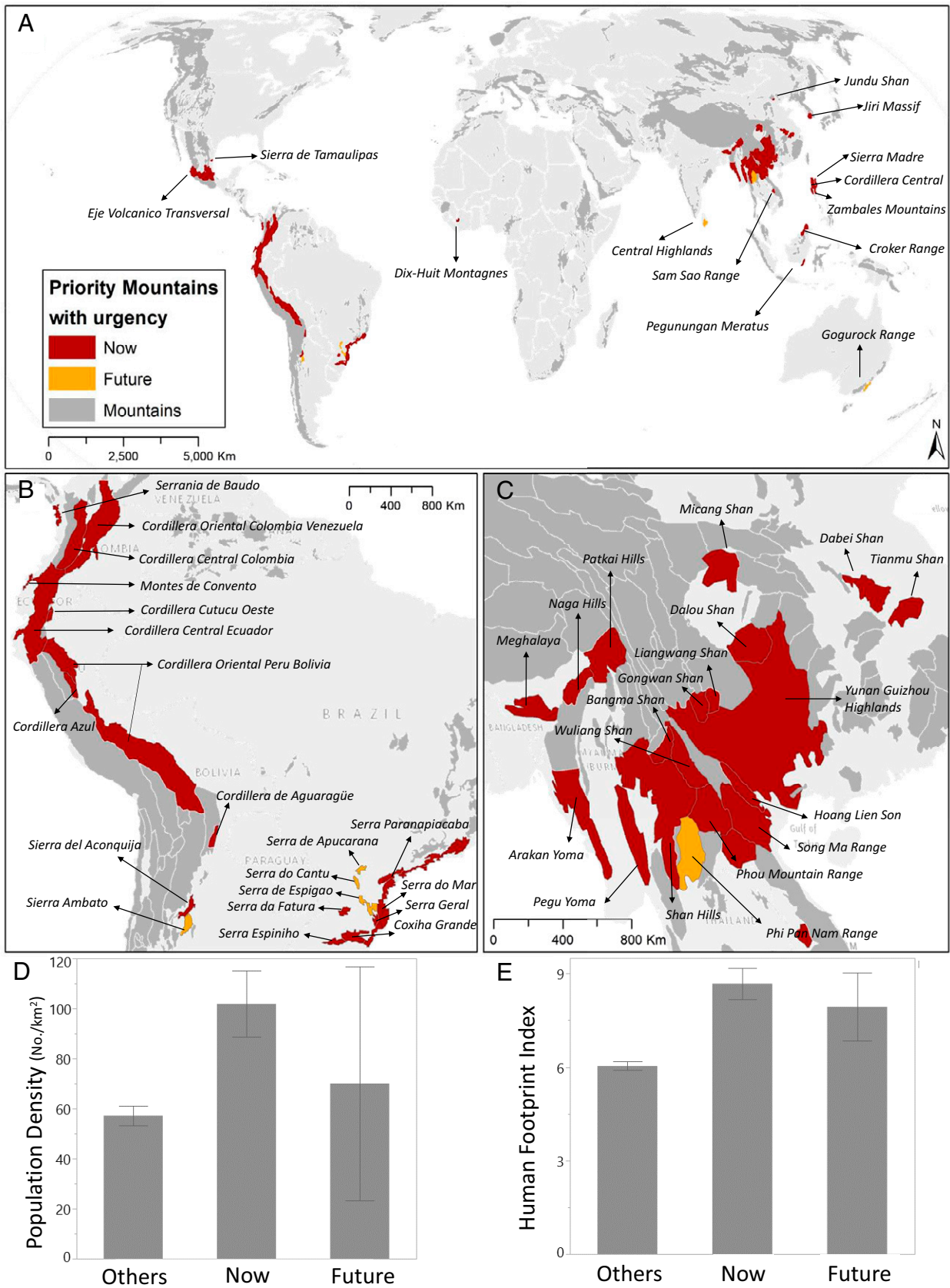


Fig. 6. Priority mountains with high urgency for immediate conservation actions. (A) Global distribution of current priority mountains with high urgency (Current: 45 mountains) and future priority mountains with high urgency (Future: seven mountains). Enlarged maps for South America (B) and Asia (C). Population density (D) and human footprint index (E) in different mountain categories, Current ($n = 45$), Future ($n = 7$) priority mountains, and all the other mountains (Others).

would not only protect the mountain biodiversity, reduce deforestation, and allow faster forest regeneration, it could also provide a nature-based solution for risk reduction around communities that are vulnerable to landslides and other natural hazards (54).

Materials and Methods

Biodiversity. We used vertebrate species as our representative for biodiversity. Species distribution data for mammals, birds, and amphibians were from the International Union for Conservation of Nature (IUCN) Red List website (40). We calculated rarity-weighted richness for each taxon to indicate the potential irreplaceability of a region (55). A cell size of 10×10 km was used across terrestrial ecosystems for the whole globe.

Rarity-weighted richness prioritizes regions with high numbers of limited range species and sometimes is identified as weighted endemism (41, 42). We calculated rarity-weighted richness using the following equation (42, 56):

$$\text{Rarity Weighted Richness} = \sum_{i=1}^n \frac{1}{r_i}$$

where r_i is the range size of a species i . The rarity-weighted richness for a given pixel is summed for the n species that occur in the pixel. Because of limited studies on certain species, some species had a single locality with an arbitrarily sized circle around it as its range. To reduce the distortion caused by this phenomenon and some other extremely small-ranged species for any species with a range size smaller than 100 km^2 , we weighted it as if it were 100 km^2 .

Landslide Susceptibility. We used a global landslide susceptibility map to locate regions that are more likely to be impacted by landslide activities. This map integrated five explanatory variables affecting the chances of landslide events, including slope, distance to faults, geological classification, presence of roads, and forest loss (28). Apart from comparing the spatial pattern visually, we also quantified the correlation with biodiversity. We quantified the correlation between biodiversity and landslide susceptibility by creating a set of random points with each at least 25 km apart to minimize the effects of spatial autocorrelation. We then extracted values of rarity-weighted richness and landslide susceptibility at each point. A t test was applied to test whether there were significant differences between biodiversity indexes in different landslide susceptible areas.

Mountain Delineation. Active research has been focusing on the definition of mountains and global mapping of mountain ranges or regions (31, 57–59). Here, we used the data from the Global Mountain Biodiversity Assessment (https://www.gmba.unibe.ch/services/tools/mountain_inventory). This dataset is based on Korner et al. (58), which used ruggedness as the main measurement to distinguish mountains and identifies 1,048 mountain ranges in the world.

Protected Areas. We extracted protected area information from the World Database of Protected Areas (available at <https://www.protectedplanet.net>) and substituted the part for China with more complete data from Pimm et al. (60). The combined dataset held information such as location, size, year of establishment, and protection category based on IUCN. We only kept the protected areas larger than 1 km^2 to exclude extremely small, protected areas and ones without area information, and we also excluded protected areas without IUCN designations. For each mountain range, we calculated the percentage covered by protected areas. We classified protected area coverage into five categories: <10%, 10 to 17%, 17 to 30%, 30 to 50%, 50 to 75%, and 75 to 100%. These thresholds represent the Aichi target of 17% for terrestrial ecosystems, 30% for a possible post-2020 target, and 50% for the half-earth goal. We used 10% to represent the minimum amount that is considered adequate for biodiversity protection (61).

Mountains with Vulnerability. We identified mountains with high vulnerability as those that are high for both biodiversity and landslide susceptibility. These areas are sensitive to anthropogenic activities, such as deforestation, agriculture expansion, and infrastructure building. Such activities not only lead to biodiversity loss but also expose people to a higher probability of landslides. We gave ranks for each mountain range according to the mean rarity score for each taxon. If the mean rarity value was larger than the 90th percentile, then a score of 5 was assigned. From 75th to 90th percentile, a score of 4 was assigned. From 50th to 75th percentile, a score of 3 was assigned. From 25th to 50th quantile, 1 was assigned. We then averaged the scores from the three taxa to get the biodiversity index for each mountain (*SI Appendix, Table 1*).

We calculated the average and majority value of landslide susceptibility for each mountain range. We assigned a score of 5 to regions with an average value larger than 4 and a score of 4 to areas with an average value larger than 3. For areas with a mean smaller than 3, if the majority value equaled 5 or 4, we assigned the score of 3. If the majority value equaled 3, we assigned a score of 1. The rest were all 0 (Fig. 3).

We ranked the mountains according to the score of both biodiversity and current landslide susceptibility. A status of vulnerable was assigned to mountains with both biodiversity and landslide scores larger or equal to 4.

Mountains with Increasing Vulnerability.

Threats from deforestation. Deforestation could increase the occurrence of landslides, further threatening the survival of species and people that inhabit mountain ecosystems. Therefore, we estimated past and future forest-cover changes for each mountain. We calculated past forest-cover change from 2000 to 2018 using Global Land Cover Maps version 2.1 from European Space Agency Climate Change Initiative (<http://maps.elie.ucl.ac.be/CCI/viewer/download.php>). We classified land-cover types, 50 to 100, 160, and 170 in the original dataset, as forests in our analysis. We derived future forest change till 2100 using the dataset from Li et al. (44). This land-cover projection dataset contains four major scenarios from The Intergovernmental Panel on Climate Change Special Report on Emissions Scenarios (44). We used the B2 Scenario, which represents the worst projection for forest-cover change (44), calculating the forest loss for each mountain.

Threats from climate change. Extensive research has been done to identify the rainfall thresholds to trigger landslides, including different indices to identify precipitation extremes. We used the following indices, RX5day, R95p, ALTCWD, and R20mm, which have been used to indicate potential risks for landslides (45–47). RX5day measures the 5-d precipitation accumulations that represent the most extreme precipitation over a 5-d period (62). This index is relevant to the landslides that may be caused by a gradual buildup of soil moisture and groundwater (45). Very wet day precipitation (R95p) measures annual total precipitation in the days with daily precipitation larger than the 95th percentile of the 1961 to 1990 daily precipitation. This index considers local historical conditions and precipitation climatologies rather than just using a single global threshold to define extreme precipitation (62). Very heavy precipitation days (R20mm) measures total days in a year with daily precipitation larger than 20 mm, indicating the frequency that landslides are possible (45). ALTCWD measures the maximum consecutive wet days that have daily precipitation larger than 1 mm, addressing the possibility of some landslides driven more by duration than the intensity of rainfall (45).

We calculated the mean for ensemble data of 48 members for each index produced with the worst climate scenario CMIP5 RCP85 (<https://climexp.knmi.nl>). Then, we calculated average values of these indices in each mountain range for each year in two periods, 1980 to 2019 and 2061 to 2100. A t test was applied to examine if each index was significantly changed across these two periods. If a mountain range had a significant increase of an index, we assigned the value 1 for that index. Then, we summed the values to form the precipitation extreme change indicator, which ranged from 0 to 4. The larger the indicator is, the more the landslide risk is predicted to increase in the future.

In addition to the mountains identified as current vulnerable mountains, we further included mountains with high biodiversity (biodiversity score ≥ 4) and moderate-landslide susceptibility ($=1$ or 3) as candidates for becoming vulnerable in the future, because of deforestation and climate change. Future deforestation could increase their landslide susceptibility levels, and increasing extreme precipitation would incur more landslide events. For these candidates, if the projected forest loss was larger than 10% of the area, then it was identified as a mountain with increasing vulnerability in the future. If the forest loss was between 1 and 10% and the precipitation extreme indicator ≥ 2 , then it was upgraded to a future priority as well.

Anthropogenic activities. We obtained population density data from the Gridded Population of the World Version 4 from NASA's Socioeconomic Data and Applications Center (63). We used the year 2020 for our analysis, which has a resolution of 1 km at the equator. We acquired the human footprint index from Venter et al. (48) and used the data for the year 2009.

ArcGIS 10.5 and JMP Pro were used for analyses.

Data Availability. All study data are included in the article and/or *SI Appendix*.

ACKNOWLEDGMENTS. Financial support for this work was provided by the China National Science Foundation (Grant 31800394) and the Strategic Priority Research Program of the Chinese Academy of Sciences (XDA19050500).

1. K. C. Seto, B. Güneralp, L. R. Hutrya, Global forecasts of urban expansion to 2030 and direct impacts on biodiversity and carbon pools. *Proc. Natl. Acad. Sci. U.S.A.* **109**, 16083–16088 (2012).
2. S. L. Maxwell, R. A. Fuller, T. M. Brooks, J. E. M. Watson, Biodiversity: The ravages of guns, nets and bulldozers. *Nature* **536**, 143–145 (2016).
3. S. Díaz *et al.*, *Summary for Policymakers of the Global Assessment Report on Biodiversity and Ecosystem Services of the Intergovernmental Science-Policy Platform on Biodiversity and Ecosystem Services* (Intergovernmental Science-Policy Platform on Biodiversity and Ecosystem Services, 2019).
4. T. Glade, Landslide occurrence as a response to land use change: A review of evidence from New Zealand. *Catena* **51**, 297–314 (2003).
5. N. Grima, D. Edwards, F. Edwards, D. Petley, B. Fisher, Landslides in the Andes: Forests can provide cost-effective landslide regulation services. *Sci. Total Environ.* **745**, 141128 (2020).
6. FAO, *Why Invest in Sustainable Mountain Development?* (FAO, Rome, Italy, 2011).
7. R. Sidle, H. Ochiai, *Landslides: Processes, Prediction, and Land Use* (American Geophysical Union, Washington, DC, 2006).
8. M. Guns, V. Vanacker, Shifts in landslide frequency–area distribution after forest conversion in the tropical Andes. *Anthropocene* **6**, 75–85 (2014).
9. L. Pisano, V. Zuppano, Ž. Malek, C. M. Rosskopf, M. Parise, Variations in the susceptibility to landslides, as a consequence of land cover changes: A look to the past, and another towards the future. *Sci. Total Environ.* **601–602**, 1147–1159 (2017).
10. M. J. Froude, D. N. Petley, Global fatal landslide occurrence from 2004 to 2016. *Nat. Hazards Earth Syst. Sci.* **18**, 2161–2181 (2018).
11. O. Kjekstad, L. Highland, “Economic and social impacts of landslides” in *Landslides—Disaster Risk Reduction*, K. Sassa, P. Canuti, Eds. (Springer, 2009), pp. 573–587.
12. D. Sanderson, A. Sharma, *World Disasters Report 2016. Resilience: Saving Lives Today, Investing for Tomorrow* (International Federation of Red Cross and Red Crescent Societies, 2016).
13. F. Guzzetti, S. Peruccacci, M. Rossi, C. P. Stark, The rainfall intensity–duration control of shallow landslides and debris flows: An update. *Landslides* **5**, 3–17 (2008).
14. M. J. Crozier, Deciphering the effect of climate change on landslide activity: A review. *Geomorphology* **124**, 260–267 (2010).
15. S. Segoni, L. Picciullo, S. L. Gariano, A review of the recent literature on rainfall thresholds for landslide occurrence. *Landslides* **15**, 1483–1501 (2018).
16. P. A. O’Gorman, Precipitation extremes under climate change. *Curr. Clim. Change Rep.* **1**, 49–59 (2015).
17. T. F. Stocker, *Climate Change 2013: The Physical Science Basis. Contribution of Working Group I to the Fifth Assessment Report of the Intergovernmental Panel on Climate Change* (Intergovernmental Panel on Climate Change, 2013).
18. E. M. Fischer, R. Knutti, Observed heavy precipitation increase confirms theory and early models. *Nat. Clim. Chang.* **6**, 986–991 (2016).
19. G. Myhre *et al.*, Frequency of extreme precipitation increases extensively with event rareness under global warming. *Sci. Rep.* **9**, 16063 (2019).
20. B. C. O’Neill *et al.*, IPCC reasons for concern regarding climate change risks. *Nat. Clim. Chang.* **7**, 28–37 (2017).
21. S. L. Gariano, F. Guzzetti, Landslides in a changing climate. *Earth Sci. Rev.* **162**, 227–252 (2016).
22. D. Kirschbaum, S. Kapnick, T. Stanley, S. Pascale, Changes in extreme precipitation and landslides over High Mountain Asia. *Geophys. Res. Lett.* **47**, e2019GL085347 (2020).
23. I. Palomo, Climate change impacts on ecosystem services in high mountain areas: A literature review. *Mt. Res. Dev.* **37**, 179–187 (2017).
24. P. Gentle, T. N. Maraseni, Climate change, poverty and livelihoods: Adaptation practices by rural mountain communities in Nepal. *Environ. Sci. Policy* **21**, 24–34 (2012).
25. A. Schild, ICIMOD’s position on climate change and mountain systems. *Mt. Res. Dev.* **28**, 328–331 (2008).
26. J. Loeffler *et al.*, Mountain ecosystem response to global change. *Erdkunde* **65**, 189–213 (2011).
27. L. Highland, P. T. Bobrowsky, *The Landslide Handbook: A Guide to Understanding Landslides* (US Geological Survey Reston, 2008).
28. T. Stanley, D. B. Kirschbaum, A heuristic approach to global landslide susceptibility mapping. *Nat. Hazards (Dordr)* **87**, 145–164 (2017).
29. R. C. Sidle, W. H. Benson, J. F. Carriger, T. Kamai, Broader perspective on ecosystem sustainability: Consequences for decision making. *Proc. Natl. Acad. Sci. U.S.A.* **110**, 9201–9208 (2013).
30. C. Hoorn, A. Perrigo, A. Antonelli, *Mountains, Climate and Biodiversity* (John Wiley & Sons, 2018).
31. C. Rahbek *et al.*, Building mountain biodiversity: Geological and evolutionary processes. *Science* **365**, 1114–1119 (2019).
32. D. Payne, E. M. Spehn, M. Sneathlage, M. Fischer, Opportunities for research on mountain biodiversity under global change. *Curr. Opin. Environ. Sustain.* **29**, 40–47 (2017).
33. A. Grêt-Regamey, S. H. Brunner, F. Kienast, Mountain ecosystem services: Who cares? *Mt. Res. Dev.* **32**, 523–534 (2012).
34. J. Liu, Z. Ouyang, H. Miao, Environmental attitudes of stakeholders and their perceptions regarding protected area–community conflicts: A case study in China. *J. Environ. Manage.* **91**, 2254–2262 (2010).
35. K. Brown, Innovations for conservation and development. *Geogr. J.* **168**, 6–17 (2002).
36. S. L. Gariano, G. Rianna, O. Petrucci, F. Guzzetti, Assessing future changes in the occurrence of rainfall-induced landslides at a regional scale. *Sci. Total Environ.* **596–597**, 417–426 (2017).
37. P. Lehmann, J. von Ruetten, D. Or, Deforestation effects on rainfall-induced shallow landslides: Remote sensing and physically-based modelling. *Water Resour. Res.* **55**, 9962–9976 (2019).
38. S. Keesstra *et al.*, The superior effect of nature based solutions in land management for enhancing ecosystem services. *Sci. Total Environ.* **610–611**, 997–1009 (2018).
39. E. Cohen-Shacham, G. Walters, C. Janzen, S. Maginnis, *Nature-Based Solutions to Address Global Societal Challenges* (IUCN, Gland, Switzerland, 2016).
40. IUCN, The IUCN Red List of Threatened Species, Version 2020-2. <https://www.iucnredlist.org>. Accessed on 1 August 2020. (2020).
41. B. A. Stein, L. S. Kutner, G. A. Hammerson, L. L. Master, L. E. Morse, “State of the states: Geographic patterns of diversity, rarity, and endemism” in *Precious Heritage: The Status of Biodiversity in the United States*, B. Stein, L. S. Kutner, J. S. Adams, Eds. (Oxford University Press, New York, 2000), pp. 119–158.
42. F. Albuquerque, P. Beier, Global patterns and environmental correlates of high-priority conservation areas for vertebrates. *J. Biogeogr.* **42**, 1397–1405 (2015).
43. ESA, Global Land Cover Maps version 2.1. <http://maps.elie.ucl.ac.be/CC/Lviewer/download.php>.
44. X. Li *et al.*, A new global land-use and land-cover change product at a 1-km resolution for 2010 to 2100 based on human–environment interactions. *Ann. Assoc. Am. Geogr.* **107**, 1040–1059 (2017).
45. T. Stanley, D. B. Kirschbaum, S. Pascale, S. Kapnick, “Extreme precipitation in the Himalayan landslide hotspot” in *Satellite Precipitation Measurement* (Springer, 2020), pp. 1087–1111.
46. J. Cepeda, K. Höeg, F. Nadim, Landslide-triggering rainfall thresholds: A conceptual framework. *Q. J. Eng. Geol. Hydrogeol.* **43**, 69–84 (2010).
47. J. Chen, W. Huang, C. Jan, Y. Yang, Recent changes in the number of rainfall events related to debris-flow occurrence in the Chenyulan Stream Watershed, Taiwan. *Nat. Hazards Earth Syst. Sci.* **12**, 1539–1549 (2012).
48. O. Venter *et al.*, Sixteen years of change in the global terrestrial human footprint and implications for biodiversity conservation. *Nat. Commun.* **7**, 12558 (2016).
49. J. Handmer *et al.*, “Changes in impacts of climate extremes: Human systems and ecosystems” in *Managing the Risks of Extreme Events and Disasters to Advance Climate Change Adaptation: Special Report of the Intergovernmental Panel on Climate Change*, C. B. Field *et al.*, Eds. (Cambridge University Press, 2012), pp. 231–290.
50. R. A. Vaidya *et al.*, “Disaster risk reduction and building resilience in the Hindu Kush Himalaya” in *The Hindu Kush Himalaya Assessment*, P. Wester, A. Mishra, A. Mukherji, A. B. Shrestha, Eds. (Springer, 2019), pp. 389–419.
51. F. Hua *et al.*, Opportunities for biodiversity gains under the world’s largest reforestation programme. *Nat. Commun.* **7**, 12717 (2016).
52. B. C. Nicoll, B. A. Gardiner, B. Rayner, A. J. Peace, Anchorage of coniferous trees in relation to species, soil type, and rooting depth. *Can. J. For. Res.* **36**, 1871–1883 (2006).
53. N. Nilaweera, P. Notalaya, Role of tree roots in slope stabilisation. *Bull. Eng. Geol. Environ.* **57**, 337–342 (1999).
54. N. Ocampo-Peñuela, S. L. Pimm, Bird conservation would complement landslide prevention in the Central Andes of Colombia. *PeerJ* **3**, e779 (2015).
55. R. Pressey, Applications of irreducibility analysis to planning and management problems. *Parks* **9**, 42–51 (1999).
56. P. Williams *et al.*, A comparison of richness hotspots, rarity hotspots, and complementary areas for conserving diversity of British birds. *Conserv. Biol.* **10**, 155–174 (1996).
57. C. Körner, J. Paulsen, E. M. Spehn, A definition of mountains and their bioclimatic belts for global comparisons of biodiversity data. *Alp. Bot.* **121**, 73–78 (2011).
58. C. Körner *et al.*, A global inventory of mountains for bio-geographical applications. *Alp. Bot.* **127**, 1–15 (2017).
59. R. Sayre *et al.*, A new high-resolution map of world mountains and an online tool for visualizing and comparing characterizations of global mountain distributions. *Mt. Res. Dev.* **38**, 240–249 (2018).
60. S. L. Pimm, C. N. Jenkins, B. V. Li, How to protect half of Earth to ensure it protects sufficient biodiversity. *Sci. Adv.* **4**, eaat2616 (2018).
61. B. V. Li, S. L. Pimm, China’s endemic vertebrates sheltering under the protective umbrella of the giant panda. *Conserv. Biol.* **30**, 329–339 (2016).
62. J. Sillmann, V. V. Kharin, F. Zwiers, X. Zhang, D. Bronaugh, Climate extremes indices in the CMIP5 multimodel ensemble: Part 2. Future climate projections. *J. Geophys. Res. D Atmospheres* **118**, 2473–2493 (2013).
63. Center for International Earth Science Information Network - CIESIN - Columbia University, *Gridded Population of the World, Version 4 (GPWv4): Population Density, Revision 11* (NASA Socioeconomic Data and Applications Center, Palisades, NY, 2018).